

## The uptake of silica during the spring bloom in the Northeast Atlantic Ocean

*Louise Brown*<sup>1</sup>

Queen's University Belfast Marine Laboratory, 12–13 The Strand, Portaferry, County Down, BT22 1PF, UK

*Richard Sanders*

George Deacon Division, Southampton Oceanography Centre, Waterfront Campus, Empress Dock, Southampton, SO14 3ZH, UK

*Graham Savidge*

Queen's University Belfast Marine Laboratory, 12–13 The Strand, Portaferry, County Down, BT22 1PF, UK

*Cathy H. Lucas*

School of Ocean and Earth Sciences, Southampton Oceanography Centre, Waterfront Campus, Empress Dock, Southampton, SO14 3ZH, UK

### *Abstract*

A full understanding of the biogeochemical cycling of silica in the North Atlantic is hampered by a lack of estimates of silica uptake by phytoplankton. We applied the <sup>32</sup>Si radiotracer incubation technique to determine silica uptake rates at 10 sites during the UK-(Natural Environment Research Council) Faroes–Iceland–Scotland hydrographic and environmental survey (FISHES) cruise in the Northeast Atlantic, May 2001. Column silica uptake rates ranged between 6 and 166 mmol Si m<sup>-2</sup> d<sup>-1</sup>; this data set was integrated with concurrent hydrographic, chemical, and primary productivity data to explain these changes in silica uptake in terms of the progress of the spring bloom. In order to interpret data covering a relatively large spatial and temporal scale, we used mean photic zone silica concentration as a proxy time-series measure of diatom bloom progression. Both absolute and specific silica uptake rates were highest at dissolved silica concentrations >2 μmol L<sup>-1</sup>. Si and C uptake were vertically decoupled at those stations where surface silica was strongly depleted. Absolute primary productivity was not strongly correlated with dissolved silica concentrations, owing to either exhaustion of silica at diatom-dominated stations or to dominance of the community by other phytoplankton. Silica uptake as a function of increased substrate concentration was linear up to 25 μmol L<sup>-1</sup>; we consider some possible reasons for the nonhyperbolic response.

The North Atlantic has long been regarded as a key area for the study of the biogeochemical cycling of carbon and nutrients in the ocean. The importance of this area relates to the high rates of primary production, nutrient uptake, and cycling associated with the annual spring bloom, which develops in response to vertical stratification of the water column (Ducklow and Harris 1993). Primary production at this time is frequently dominated by diatoms (Savidge et al. 1995), and, as a consequence of their relatively large size and rapid sinking rate, they also play an important role in the export of biological materials to the deep ocean (Honjo

and Manganini 1993). As the primary users of dissolved inorganic silica, diatoms' rates of silica uptake and the subsequent dissolution of their frustules exert a major control on the oceanic silica cycle. As the spring bloom progresses, depletion of the surface silica pool by diatom uptake often results in limitation of diatom growth rates, and this has been proposed as the cause for the eventual collapse of the bloom (Martin-Jezequel et al. 2000).

Quantitative determination of Si and C uptake by diatoms and the associated export fluxes are vital for understanding marine biogeochemical cycles and the initiation and evolution of phytoplankton blooms (e.g., Pondaven et al. 1999). Estimates of silica uptake have previously been obtained from marine environments with diverse hydrography, nutrient supply, and insolation regimes. Integrated silica uptake rates vary from <0.5 mmol Si m<sup>-2</sup> d<sup>-1</sup> in oligotrophic mid-ocean gyres (Brzezinski and Kosman 1996; Nelson and Brzezinski 1997) to >200 mmol Si m<sup>-2</sup> d<sup>-1</sup> in coastal upwelling blooms (Nelson and Goering 1978; Brzezinski et al. 1997).

In most marine environments, the rate of silica uptake is controlled primarily by the concentration and supply of inorganic silica in the surface ocean. Thus, intense diatom blooms are observed in the nutrient-rich waters of the Southern Ocean and adjoining marginal seas (e.g., Smith et al.

<sup>1</sup> Present address: George Deacon Division, Southampton Oceanography Centre, Waterfront Campus, Empress Dock, Southampton, SO14 3ZH, UK.

### *Acknowledgments*

This work was supported through UK Natural Environment Research Council small grant NER/B/S/2000/00815 awarded to Queen's University Belfast. We thank the captain and crew of RRS *Discovery* cruise D253 for their assistance on the cruise. The FISHES scientific team provided ancillary data and helpful comments throughout the preparation of the manuscript; particular thanks go to Mike Lucas, Mark Moore, Tim O'Higgins, and Russell Davidson for phytoplankton pigment data and taxonomy, and John Allen for physical data. We also thank two anonymous referees for their invaluable comments on the manuscript.

1999; Nelson et al. 2001; Queguiner and Brzezinski 2002), with maximum silica uptake rates of 40–60 mmol Si m<sup>-2</sup> d<sup>-1</sup>. In contrast, the highest rates in the oligotrophic subtropical Atlantic Ocean are of the order of 2–3 mmol Si m<sup>-2</sup> d<sup>-1</sup>. In the high nitrate–low chlorophyll (HNLC) regions of the Southern Ocean, winter mixing raises surface Si concentrations to >40 μmol L<sup>-1</sup>, which is subsequently used by diatoms maintained in the surface ocean by thermal and density-driven stratification in spring (e.g., Brzezinski et al. 2001). The bloom continues until exhaustion of surface nutrients limits diatom growth or mixing removes the diatom population from the photic zone. In contrast, silica concentration in the oligotrophic subtropical Atlantic waters reaches a maximum of 2–3 μmol L<sup>-1</sup> following winter mixing, and uptake rates in the winter/spring bloom of this region are much lower (Brzezinski and Kosman 1996; Nelson and Brzezinski 1997). Periods of peak diatom activity in the central North Pacific are driven not only by winter upwelling, but by cyclonic eddy activity throughout the year (Brzezinski et al. 1998). In equatorial regions, diatom growth is also associated with upwelling (Leynaert et al. 2001).

In both high- and low-nutrient environments, there is evidence from kinetic studies of silica limitation of diatom productivity (Brzezinski and Nelson 1996; Franck et al. 2000; Leynaert et al. 2001; Nelson et al. 2001). It had been anticipated that open ocean diatom assemblages would have a greater affinity for silica (i.e., a lower half-saturation constant) in regions of low surface [Si(OH)<sub>4</sub>] than observed in areas where silica was readily available, as a response to the reduced substrate availability. This was confirmed by observations in low silica warm-core rings in the Atlantic Gulf Stream (Nelson and Brzezinski 1990). However, some of the most inefficient (relative to ambient silica concentrations) uptake kinetics have been observed in the oligotrophic Sargasso Sea (Brzezinski and Nelson 1996) and central North Pacific (Brzezinski et al. 1998). Evidence for enhancement of silica uptake by addition of the micronutrients Fe and Zn has also been reported for the Southern Ocean (Boyd et al. 1999; Franck et al. 2000) and Pacific Ocean (Leynaert et al. 2001). However, enhanced input of iron-rich Aeolian dust to the Sargasso Sea provoked no increase in silica uptake by diatoms, indicating it is unlikely to be a limiting factor in the subtropical Atlantic (Nelson and Brzezinski 1997).

Studies in both the Southern Ocean (Smith et al. 1999; Brzezinski et al. 2001) and the equatorial Pacific (Leynaert et al. 2001) have found that silica uptake rates decrease to effectively zero at the base of the photic zone, implying a degree of vertical coupling of Si : C uptake. However, in other regions, experimental evidence indicates a stronger potential control of dissolved silica concentration on the distribution of silica uptake rates throughout the water column. For example, significant silica use was observed at the base of and below the nitracline in the Weddell-Scotia Seas (Treguer et al. 1991), Sargasso Sea (Brzezinski and Nelson 1996; Brzezinski and Kosman 1996) and central North Pacific (Brzezinski et al. 1998). Thus, the strong light dependence of both carbon and nitrogen uptake cannot unequivocally be assumed for silica uptake.

At present there is an absence of data on diatom production and silica uptake kinetics in the open Northeast Atlantic

ocean. The annual silica cycle here is characterized by a transition from silica concentrations of about 6–8 μmol L<sup>-1</sup> in winter to concentrations of about 1 μmol L<sup>-1</sup> or less (Louanchi and Najjar 2001), potentially limiting diatom production. In such regions we hypothesize that silica depletion should be the major control on silica uptake and diatom bloom progression. Consequently, silica uptake rates and diatom growth rates would be expected to be greatest at the initiation of the spring bloom, when dissolved silica concentration is still high, then decline as surface silica is depleted. Second, we hypothesize that silica limitation of an actively growing surface layer diatom population may result in use of the subphotic zone silica pool, as observed in the Pacific and Atlantic oceanic gyres (Brzezinski and Nelson 1996; Brzezinski and Kosman 1996; Brzezinski et al. 1998).

In this study we test these two hypotheses using Si uptake and diatom production data acquired in the Northeast Atlantic during the spring phytoplankton bloom. The annual silica cycle in surface waters of this region is driven by deep winter mixing to 800–1,000 m, which increases surface silica concentration to 4–7 μmol L<sup>-1</sup> (Koeve 2001; Louanchi and Najjar 2001), which is then depleted by the spring diatom bloom. Thus this region is an appropriate environment in which to examine the impact of a spring bloom-driven transition from silica richness to silica depletion on diatom silica uptake rates. Our data were obtained as part of the multi-disciplinary FISHES (Faeroes–Iceland–Scotland hydrographic and environmental survey) cruise investigating the ecosystem response to mesoscale dynamics in the Iceland Basin, which took place in May and June 2001.

Conventional techniques for determining silica uptake rates by marine phytoplankton require addition of the stable isotope <sup>30</sup>Si to seawater samples, followed by determination of the <sup>30</sup>Si : <sup>28</sup>Si ratio of particulate material by mass spectrometry (Nelson and Goering 1977). This approach is inappropriate for North Atlantic waters, since the addition of <sup>30</sup>Si tracer required is comparable with the ambient silica concentrations, resulting in enhanced rates of diatom silica uptake in tracer studies relative to natural conditions. However, the development of a sensitive radiotracer method using a high specific activity solution of <sup>32</sup>Si eliminates this difficulty, enabling rapid, high-precision analysis while increasing ambient dissolved silica concentrations by only a few nanomoles (Brzezinski and Phillips 1997).

We applied this method to determine silica uptake rates on a series of depth profiles and examine uptake kinetics at another four stations. The results are considered in the context of the hydrographic and chemical characteristics of each site, which we use to synthesize a quasi-time series of silica uptake through the spring diatom bloom.

## Methods

*Sampling and study area*—All fieldwork was carried out during the first leg of the FISHES cruise (RRS *Discovery* cruise D253), from 4 to 31 May 2001. One station each day was selected for detailed study of the plankton community; the timing of this station was such that sample collection was as close to dawn as possible. Temperature and salinity

profiles for each station were determined from calibrated conductivity-temperature-depth (CTD) data, collected using either a Neil Brown MkIII or a Sea-Bird 911 CTD package. Seawater was collected in 20-liter Go-Flo bottles mounted on a rosette sampler from seven depths within the euphotic zone, corresponding to 97%, 45%, 17.6%, 8.0%, 2.9%, 1.3%, and 0.1% of the intensity of surface photosynthetically active radiation (PAR). These depths were determined from a PAR sensor on a Chelsea Instruments fast repetition rate fluorometer, deployed immediately prior to the CTD cast. Planktonic silica uptake was measured at 10 of these stations and silica uptake kinetics at a further four stations.

**<sup>32</sup>Si production rates**—The technique used in this study was based on that of Brzezinski and Phillips (1997), modified for shipboard work. Samples were decanted from the Go-Flo bottles into acid-washed (0.1 mol L<sup>-1</sup> HCl) and de-ionized water-rinsed 2-liter polycarbonate bottles and prepared for incubation immediately after collection under minimal light conditions. Three 250-ml polycarbonate bottles were rinsed twice with the sample, filled, and inoculated with 1.11 MBq (0.03 μCi) of a high specific activity (7.77 MBq/2.1 μCi ml<sup>-1</sup>) <sup>32</sup>Si tracer (Los Alamos National Laboratory) diluted in an artificial seawater solution, using a Wheaton positive displacement pipette. Another bottle, wrapped in aluminum foil to exclude light, was also incubated at each depth to examine uptake under dark conditions. Uptake of <sup>32</sup>Si by inorganic particles has been shown to be insignificant (Leynaert et al. 2001); thus, no correction for inorganic uptake of <sup>32</sup>Si was considered necessary.

The <sup>32</sup>Si-spiked sample bottles were incubated for 6 h in continuously flowing surface seawater. Six hour incubations were preferred to 24-h incubations, in order to avoid nutrient exhaustion or silica remineralization compromising the uptake rate measurements. We therefore ensured the incubations were conducted between 0600 h and 1200 h to obtain a value for a half-day cycle. The deck incubators were covered with combinations of blue and neutral density light filters to simulate the in situ light intensity for each set of samples. Incubations were terminated by filtering through 0.8-μm polycarbonate filters under gentle vacuum, followed by three washes of GF/F-filtered seawater. Each filter was placed in a 20-ml glass scintillation vial with 2.5 ml 0.2 mol L<sup>-1</sup> NaOH and heated at 85°C for 2 h to digest the biogenic silica (Ragueneau and Treguer 1994). Digestion of total silica was not attempted due to the hazards associated with use of hydrofluoric acid at sea. After cooling, 10 ml of Optiphase HiSafe 3 (Perkin Elmer Life Sciences) scintillation cocktail was added to each vial. Samples were counted using a dual-window (channels 1–600 and 600–1010) counting protocol on an LKB-Wallac 1414 liquid scintillation counter (LSC) for 45 min or <1% precision. The counting efficiency of the isotopes in the assigned counting windows of the scintillation counter was fully calibrated using <sup>32</sup>Si and <sup>32</sup>P spikes, following the method outlined in Brzezinski and Phillips (1997). A quench curve for the <sup>32</sup>Si spike in the NaOH-Optiphase HiSafe3 counting medium was created prior to the cruise, using nitromethane as a quenching agent. Uptake rates were determined from the equation

$$\rho_{\text{Si}} = \frac{({}^{32}\text{Si}_{\text{PSi}}/{}^{32}\text{Si}_{\text{tot}}) \times [\text{Si}(\text{OH})_4]}{t} \quad (1)$$

where  $\rho_{\text{Si}}$  is the silica incorporation rate as measured by <sup>32</sup>Si uptake;  ${}^{32}\text{Si}_{\text{PSi}}$  is the activity of <sup>32</sup>Si in the filtered particulate material;  ${}^{32}\text{Si}_{\text{tot}}$  is the total activity of <sup>32</sup>Si tracer added to the incubation bottle, determined by daily standardization;  $[\text{Si}(\text{OH})_4]$  is the dissolved silicic acid concentration at the start of the incubation; and  $t$  is the duration of the incubation (Brzezinski and Phillips 1997). Biomass-normalized specific uptake rates,  $\mu_{\text{Si}}$ , were also calculated, using the following equation (Brzezinski and Phillips 1997)

$$\mu_{\text{Si}} = \ln\left(\frac{\rho_{\text{Si}} + \text{BSi}}{\text{BSi}}\right) \quad (2)$$

where  $\rho_{\text{Si}}$  is the silica uptake rate, as calculated above, and BSi is the initial particulate biogenic silica concentration in the sample.

The activity of <sup>32</sup>Si added was calibrated daily as follows: a 100-μl aliquot of <sup>32</sup>Si stock was diluted with the artificial seawater dilution solution in a 10-ml volumetric flask. Three 2.5-ml aliquots were pipetted into 20-ml glass scintillation vials and 10 ml of Optiphase HiSafe 3 scintillation cocktail added. The vials were counted by LSC as before, and the activity of the stock was standardized from the mean value of the three counts.

**<sup>32</sup>Si uptake kinetics studies**—Uptake kinetics studies were carried out at four stations (13989, 14053, 14066, and 14088), with ambient surface silica concentrations of 5.5 μmol L<sup>-1</sup>, 1.0 μmol L<sup>-1</sup>, 0.3 μmol L<sup>-1</sup>, and 1.6 μmol L<sup>-1</sup>, respectively. A single 8–10-liter water sample was collected from the depth of the maximum chlorophyll concentration as observed by the CTD fluorometer. The water was subsampled into 250-ml polycarbonate bottles, to which incremental quantities of a 1.5 μmol L<sup>-1</sup> NaSiO<sub>3</sub> solution were added to increase the dissolved silica concentration. For each series, eight additions were made, the concentrations being dependent on the ambient silica concentration of the surface water. Each concentration increment was analyzed in duplicate or triplicate, depending on the total volume of sample available. The samples were inoculated with 1.11 MBq (0.03 μCi) of <sup>32</sup>Si tracer, incubated, and processed as described above.

**Primary production**—Measurements of primary productivity using the <sup>14</sup>C technique outlined in Parsons et al. (1984, pp. 22–25) were made at all stations where <sup>32</sup>Si incubations were carried out. Subsamples from the 20-liter CTD bottles were decanted into 2-liter polycarbonate bottles as before, then four 60-ml polycarbonate bottles for each of the seven percentage PAR depths were rinsed and filled with the sample. One bottle was wrapped in aluminum foil to obtain a value for nonphotosynthetic uptake. 370 MBq (10 μCi) of <sup>14</sup>C stock solution, in an artificial seawater dilution solution, was added to each bottle and the bottles incubated under the same conditions as described for the <sup>32</sup>Si studies, thus facilitating a direct comparison between silica and carbon uptake rates. Incubations were terminated by filtering

samples under gentle vacuum through 47-mm diameter 0.2- $\mu\text{m}$  polycarbonate filters. The filters were then placed in 7-ml polyethylene vials and fumed over concentrated HCl to eliminate inorganic carbonate before being dried overnight in a desiccator containing silica gel crystals. Optiphase HiSafe 3 scintillation cocktail (2.5 ml) was added to each vial, and the vials were then capped and shaken. The samples were counted for 60 min or  $<0.1\%$  precision, using the  $^{14}\text{C}$ -DPM counting protocol on an LKB-Wallac 1414 liquid scintillation counter. The samples were stored in the LSC for a minimum of 1 h to allow decay of chemoluminescence. Daily standardization of  $^{14}\text{C}$  activity was carried out by diluting 100  $\mu\text{l}$   $^{14}\text{C}$  stock in 10-ml Carbosorb and subsampling five 100- $\mu\text{l}$  aliquots into polyethylene vials. Packard Supermix scintillation cocktail (2.5 ml) was added and the samples counted by LSC as before. Primary production in  $\text{mg C m}^{-3} \text{ h}^{-1}$  is determined from the mean of the triplicate counts minus the nonphotosynthetic uptake in the dark bottle, using the equations in Parsons et al. (1984, pp. 22–25). After consideration of day length and the period over which the incubations were carried out, daily uptake rates were estimated as twice the total uptake rate measured in the 6-hourly incubation.

**Particulate matter concentration**—Two 500-ml subsamples of seawater from each of the sampling depths were reserved for the analysis of biogenic silica (BSi) and particulate organic carbon (POC). The BSi samples were vacuum filtered onto 0.8- $\mu\text{m}$  polycarbonate filters, from which the BSi was dissolved as described for the  $^{32}\text{Si}$  incubations. The solution was neutralized with 0.1 mol  $\text{L}^{-1}$  HCl, and concentrations were determined using a Skalar Mk 2 segmented flow autoanalyzer using the method outlined in Kirkwood (1995). POC samples were filtered through GF/F filters and immediately frozen at  $-20^\circ\text{C}$  for analysis by CHN analyzer on return to shore.

**Dissolved nutrient concentrations**—Samples for inorganic nutrient analyses were drawn directly from Niskin bottles into brand new polystyrene coulter counter cups. Sample bottles were rinsed with twice their own volume of sample, capped, and stored in the dark at  $4^\circ\text{C}$  until analysis, which generally commenced within 4 h. Nitrate and nitrite (hereafter referred to as nitrate), silica, and phosphate concentrations in unfiltered water samples were analyzed using a Skalar SanPlus continuous flow autoanalyzer using standard colorimetric techniques described by Kirkwood (1995) and Sanders and Jickells (2000). We estimate the short-term precision of the nitrate, phosphate, and silica analyses to be better than  $\pm 2$ – $3\%$  based on the analysis of individual water samples from multiple Niskin bottles fired at the same nominal depth. We estimate the long-term precision of nutrient analyses over the entire cruise to be better than  $3\%$  for all nutrients, based on multiple analyses over the course of the cruise of an aged deep-water sample. The detection limit of the analyses (calculated as three times the baseline noise) were better than 0.1, 0.02, and 0.05  $\mu\text{mol L}^{-1}$  for nitrate, phosphate, and silica respectively.

**Chlorophyll analysis**—Shipboard total chlorophyll analyses for each of the light depths sampled for productivity measurements were carried out by filtering 100-ml seawater from the 20-liter Go-Flo bottles on the CTD rosette sampler onto Whatman 25-mm diameter GF/F filters. The filters were placed in 20-ml brown glass vials to which 10 ml 90% acetone was added, and the vials were placed in a freezer for 24 h. The concentration of chlorophyll extracted from the filter was measured using a Turner Designs scaling fluorometer following the protocol of Welschmeyer (1994). Chlorophyll standard solutions (Sigma) covering the range of expected chlorophyll concentration were used for calibration of the fluorometer.

**High performance liquid chromatography (HPLC) pigment analysis**—five hundred milliliters of seawater samples were collected from the CTD rosette sampler from the depths at which samples for productivity measurements were collected. These were filtered onto 25-mm Whatman GF/F filters, and the filters were frozen at  $-70^\circ\text{C}$  until return to shore. The frozen filters were extracted in 2 ml of 90% acetone using sonication (30 s) and centrifuged to remove cellular debris. An aliquot (500  $\mu\text{l}$ ) of clarified extract was mixed with 500  $\mu\text{l}$  of 1 mol  $\text{L}^{-1}$  ammonium acetate and 100  $\mu\text{l}$  injected into a ThermoFinnigan HPLC system (P2000 gradient pump, vacuum degasser, AS3000 autosampler, UV6000 diode-array detector, FL3000 fluorescence detector, SN4000 system controller) incorporating a 3- $\mu\text{m}$  Adsorbosphere column ( $3 \times 0.45$  cm, Alltech). Pigment analysis using reverse phase HPLC was performed according to Barlow et al. (1993). Data collection and integration used the Chromquest 3.0 software on a Dell computer. Pigment identity was secured through coelution with authentic pigments: chlorophyll pigments were obtained from Sigma Chemical Co.; fucoxanthin and 19'-hexanoyloxyfucoxanthin from DHI, Denmark. Further confirmation of pigment identity was provided through online diode-array spectroscopy.

## Results

**Hydrography, biomass distribution, and primary production**—The basic physical, chemical, and biological characteristics of each of the stations at which  $^{32}\text{Si}$  uptake rates or uptake kinetics were determined are identified in Table 1. There were no obvious relationships between the mixed layer or euphotic depth with either time or latitude; this is likely a result of the essentially random distribution of sampling stations. The mixed layer depth, estimated as being the depth at which the CTD temperature profile changed by  $0.2^\circ\text{C}$ , exceeded the euphotic depth at only two stations, 13984 and 14010. Surface nutrient concentrations were in the range of 0.13–11.7  $\mu\text{mol L}^{-1}$  nitrate/nitrite, 0.04–0.82  $\mu\text{mol L}^{-1}$  phosphate, and 0.3–5.53  $\mu\text{mol L}^{-1}$  silica, and in general were highest to the west of the Reykjanes Ridge. Below the nitracline, concentrations were on the order of 15  $\mu\text{mol L}^{-1}$  nitrate, 0.9  $\mu\text{mol L}^{-1}$  phosphate, and 6  $\mu\text{mol L}^{-1}$  silica.

Surface chlorophyll *a* (Chl *a*) concentrations varied by an order of magnitude, from 0.3 to  $>6$  mg Chl *a*  $\text{m}^{-3}$ . Production at five of the stations (13984, 14010, 14029, 14060, and 14078) exceeded 2000 mg C  $\text{m}^{-2} \text{ d}^{-1}$ , and these stations

Table 1. Some key hydrographic, biological, and chemical characteristics of the FISHES productivity stations sampled on cruise D253, May 2001. The thermocline depth was estimated from an 0.2°C change in temperature on the CTD profile.

Station	Location (°N, °W)	Date	Thermocline depth (m)	0.1% Surface irradiance (m)	Production (mg C m <sup>-2</sup> d <sup>-1</sup> )	Integ. Chl <i>a</i> (mg m <sup>-2</sup> )	Surface Chl <i>a</i> (mg m <sup>-3</sup> )	Surface NO <sub>3</sub> <sup>-</sup> (μmol L <sup>-1</sup> )	Surface Si(OH) <sub>4</sub> (μmol L <sup>-1</sup> )	Surface PO <sub>4</sub> <sup>-</sup> (μmol L <sup>-1</sup> )
13971	58 44 27, 16 30 00	08 May	45	50	681	56.8	1.9	3.73	0.30	0.42
13984	63 00 00, 20 00 00	11 May	75	51	2,212	254.4	5.4	8.89	1.87	0.51
13989	62 27 10, 23 49 42	12 May	5	61	1,089	114.4	2.3	11.71	5.53	0.82
13995	61 05 70, 22 39 57	13 May	18	51	940	112.4	2.7	10.35	3.42	0.77
14000	60 24 05, 19 01 64	14 May	59	99	491	72.6	0.69	8.36	0.23	0.52
14005	61 44 68, 14 58 48	15 May	10	66	312	72.0	0.53	5.78	0.88	0.38
14010	63 25 00, 16 45 00	16 May	50	33	3,208	205.1	6.6	5.55	0.72	0.30
14029	56 57 00, 08 47 00	20 May	not available	35	2,348	136.8	5.5	0.13	1.50	0.04
14053	60 26 50, 12 36 49	23 May	20	61	314	28.8	1.1	7.19	1.02	0.38
14060	62 22 10, 08 19 73	24 May	26	45	2,334	111.2	2.8	7.93	1.04	0.49
14066	64 22 62, 08 28 60	25 May	20	50	736	86.8	3.0	5.4	0.33	0.50
14071	64 35 41, 10 41 34	26 May	14	29	499	244.9	7.5	6.56	0.71	0.36
14078	61 59 06, 14 58 48	27 May	33	61	2,960	66.4	1.5	8.52	2.05	0.49
14088	62 42 84, 08 21 14	29 May	14	50	750	36.2	1.8	7.84	1.56	0.32

were provisionally identified as possible locations of the spring phytoplankton bloom. Regression analysis showed no statistically significant relationships between integrated primary production and surface nutrient concentrations, integrated Chl *a* concentrations, photic zone depth, mixed layer depth, and the ratio of photic zone:mixed layer depth.

The taxonomic nature of the mixed plankton assemblage was investigated using HPLC of chlorophyll and accessory pigments. Figure 1 shows the depth distribution profiles for some key marker pigments (Jeffrey and Vesk 1997) for all stations except 13071, for which data are unavailable. Fucoxanthin, a diatom-associated pigment, is dominant

throughout the photic zone at stations 13984, 13995, and 14060, while at stations 14000 and 14005 the community appears to be fairly mixed at the surface but diatom-dominated at depth. Stations 14071, 14010, and 14078 contain mixed phytoplankton pigment signals throughout the photic zone, whereas Sta. 14029 has a high concentration of the prymnesiophyte pigment 19'-hexanoyloxyfucoxanthin.

Diatom species distributions were examined in a single sample from the 50% light depth at each station, excluding Sta. 14000 (data not shown). *Nitzschia* spp. were dominant at most stations, accounting for 50% or greater of total diatom cell counts. The exceptions were stations 14005 and

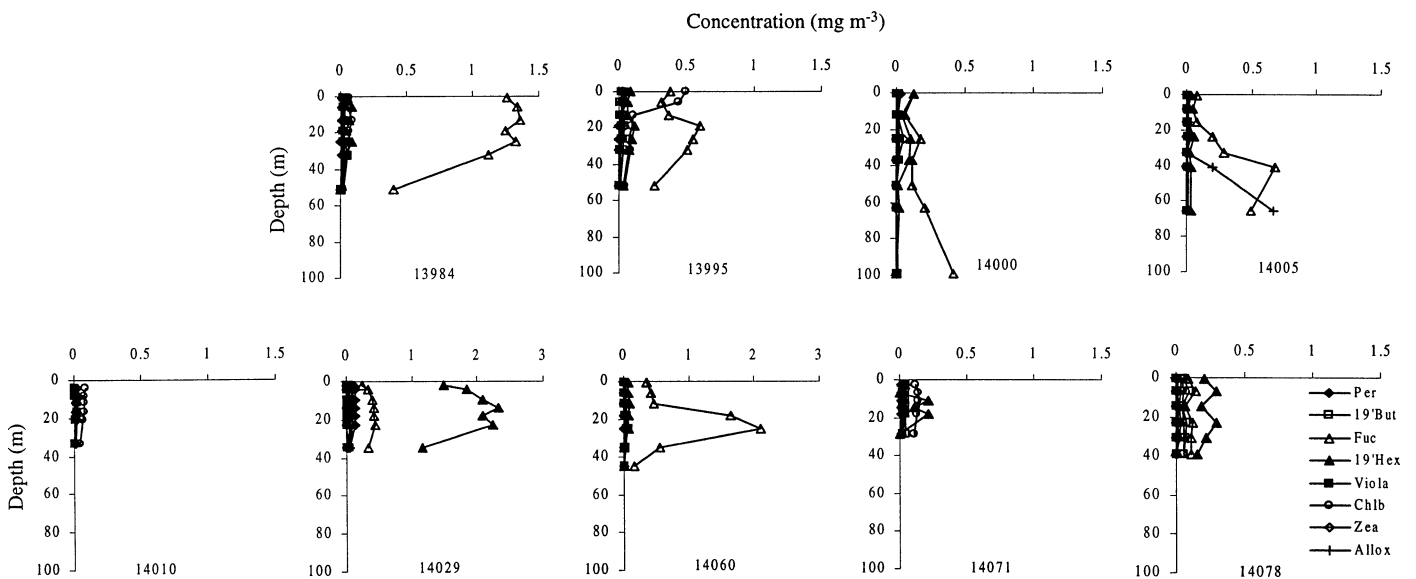


Fig. 1. Profiles of key marker pigment concentrations at the FISHES <sup>32</sup>Si study sites. Pigment abbreviations used on the figure legend are as follows: *Per*, peridinin; *19'But*, 19'-butanoyloxyfucoxanthin; *Fuc*, fucoxanthin; *19'Hex*, 19'-hexanoyloxyfucoxanthin; *Viola*, violaxanthin; *Chlb*, chlorophyll *b*; *Zea*, zeaxanthin; *Allox*, alloxanthin.

Table 2. Concentration, in  $\mu\text{mol L}^{-1}$ , of particulate organic carbon (POC) and biogenic silica (BSi) at FISHERS  $^{32}\text{Si}$  uptake sites. Si:C molar ratios are given in the fourth column. The depth-integrated values, in  $\text{mmol m}^{-2}$ , for the stations are given in italics.

Station	% PAR	POC	BSi	Si:C
13971	97	7.90	1.60	0.203
	45	9.79	1.50	0.153
	18	8.35	1.48	0.177
	8	8.97	2.08	0.232
	3	6.00	0.52	0.087
	1	7.06	0.32	0.045
	0.1	—	—	—
		<i>243</i>	<i>54</i>	<i>0.222</i>
13984	97	6.36	1.49	0.234
	45	7.79	1.98	0.254
	18	6.85	2.09	0.305
	8	5.94	1.99	0.335
	3	5.98	1.82	0.304
	1	4.11	1.52	0.370
	0.1	17.40	2.38	0.137
		<i>380</i>	<i>124</i>	<i>0.326</i>
13995	97	18.24	1.20	0.067
	45	13.05	1.16	0.089
	18	12.42	1.89	0.152
	8	12.44	2.44	0.196
	3	13.95	1.50	0.108
	1	13.99	1.17	0.084
	0.1	—	1.03	—
		<i>555</i>	<i>93</i>	<i>0.167</i>
14000	97	13.41	1.52	0.113
	45	8.65	1.13	0.131
	18	8.78	1.07	0.122
	8	10.81	0.91	0.084
	3	8.46	0.77	0.091
	1	1.73	0.51	0.295
	0.1	14.91	1.45	0.097
		<i>774</i>	<i>82</i>	<i>0.106</i>
14005	97	15.18	0.71	0.047
	45	8.50	0.50	0.059
	18	18.44	0.79	0.043
	8	17.50	0.67	0.038
	3	7.40	0.64	0.086
	1	15.26	0.80	0.052
	0.1	11.51	2.44	0.212
		<i>832</i>	<i>60</i>	<i>0.072</i>
14010	97	17.54	3.02	0.172
	45	21.12	2.73	0.129
	18	23.69	2.47	0.104
	8	31.29	2.96	0.095
	3	28.34	2.45	0.086
	1	18.13	2.54	0.140
	0.1	14.21	3.01	0.212
		<i>676</i>	<i>101</i>	<i>0.149</i>
14029	97	36.36	0.75	0.021
	45	46.86	0.63	0.013
	18	30.96	0.44	0.014
	8	32.74	0.27	0.008
	3	28.13	0.36	0.013
	1	38.27	0.43	0.011
	0.1	30.17	0.45	0.015

Table 2. Continued.

Station	% PAR	POC	BSi	Si:C
		<i>1,106</i>	<i>10.2</i>	<i>0.009</i>
14060	97	84.55	2.36	0.028
	45	17.79	1.66	0.093
	18	14.14	1.39	0.098
	8	27.14	5.30	0.195
	3	16.79	0.65	0.039
	1	6.84	1.37	0.200
	0.1	6.76	5.38	0.796
		<i>604</i>	<i>104</i>	<i>0.172</i>
14071	97	27.94	2.37	0.085
	45	25.04	2.41	0.096
	18	25.88	3.05	0.118
	8	22.22	3.14	0.141
	3	24.99	2.85	0.114
	1	17.11	2.98	0.174
	0.1	38.87	2.31	0.059
		<i>689</i>	<i>148</i>	<i>0.215</i>
14078	97	14.96	0.77	0.051
	45	29.96	0.60	0.020
	18	23.25	0.43	0.018
	8	13.07	0.41	0.031
	3	14.83	0.45	0.030
	1	14.52	0.37	0.025
	0.1	10.01	0.42	0.042
		<i>948</i>	<i>18.4</i>	<i>0.020</i>

14066 (high concentrations of both *Nitzschia* spp. and *Chaetoceros* spp.); Sta. 14029 (abundant *Nitzschia* spp., *Chaetoceros* spp., and pennate diatoms); and Stas. 13971 and 13995 (dominated by *Chaetoceros* spp.). The most diverse diatom community was observed at Sta. 14053, containing *Rhizosolenia*, *Thalassosira*, *Leptocylindrus*, and centric species in considerable numbers, in addition to *Nitzschia* spp.

Biogenic silica concentrations were of the order  $0.5\text{--}3 \mu\text{mol L}^{-1}$  throughout the water column at most stations (Table 2). At Sta. 14060, two peaks of magnitude  $5 \mu\text{mol L}^{-1}$  were observed at 8% surface PAR, approximately corresponding to the depth of the thermocline, and at 0.1% PAR. Stations 13984, 14000, and 14005 also exhibited moderate peaks at the 0.1% PAR data point, while a peak in BSi was observed just above the thermocline at Sta. 13995. POC values were typically  $10\text{--}40 \mu\text{mol L}^{-1}$ , with the exception of a single surface value of  $84 \mu\text{mol L}^{-1}$  at Sta. 14060. Peaks in POC concentration at depth were observed at Stas. 13984, 14000, and 14071. POC and BSi concentrations were integrated to the depth of the 0.1% PAR light level and ranged between 243 and 1,106  $\text{mmol m}^{-2}$  for POC (Stas. 13971 and 14029, respectively), and 10.2 and 148  $\text{mmol m}^{-2}$  for BSi (Stas. 14029 and 14071). Regression of BSi and POC with silica uptake rates and primary production, respectively, did not demonstrate any significant relationship, indicating either highly variable phytoplankton growth rates or that particulate material at some stations contained a significant detrital component. Integrated Si:C ratios varied from 0.25 to 0.012, with a mean value for all stations of  $0.055 \pm 0.044$ . Two stations (14029, 14078) deviated strongly from the data set;

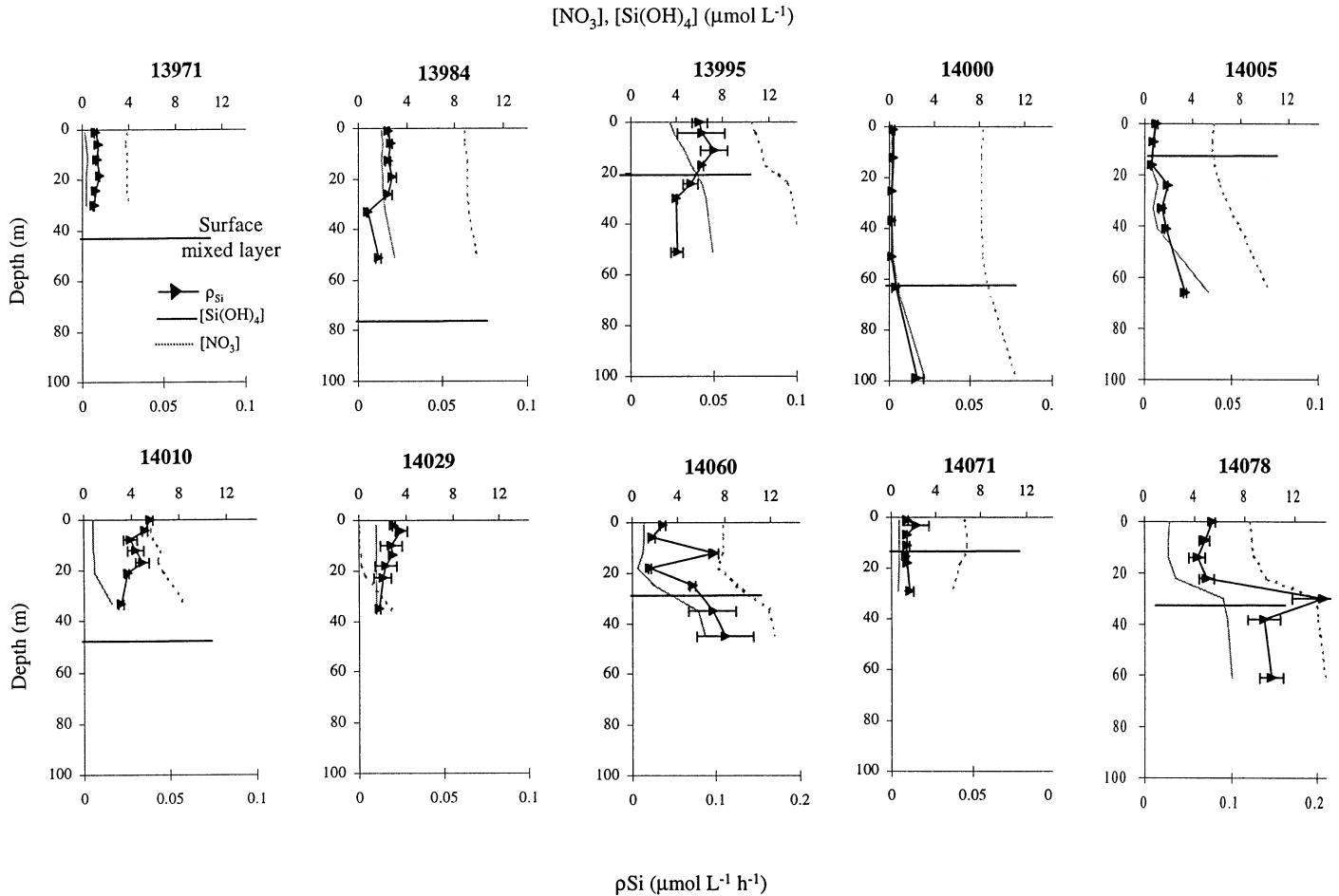


Fig. 2. Silica uptake rate profiles measured at the 10 FISHES stations. The results are the mean of three bottles incubated at each depth, and the error bars represent the standard deviation of the rates measured in the triplicate samples. The concentrations of silicate and nitrate, in  $\mu\text{mol L}^{-1}$ , are also shown. The mixed layer depth, defined by a  $0.2^\circ\text{C}$  change in temperature on the CTD profile, is also indicated.

removing these reduced the value to  $0.10 \pm 0.04$ , somewhat closer to the generally accepted value for diatom Si:C ratio of 0.13 (Brzezinski 1985).

<sup>32</sup>Si uptake profiles—The profiles of silica uptake and nitrate and silica concentrations at each of the 10 stations are

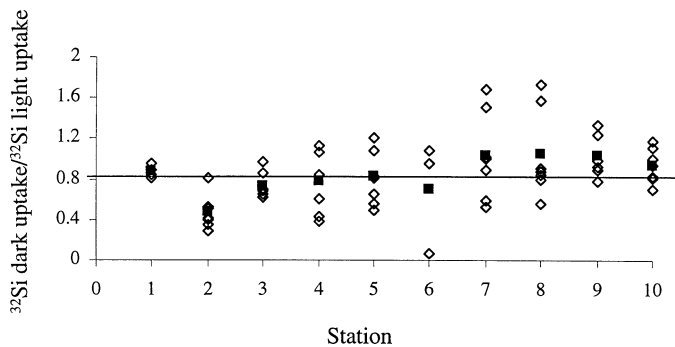


Fig. 3. Ratio of dark uptake to light uptake in samples from the same depth, incubated under identical conditions. The open symbols represent the ratios calculated for each light depth (dark bottle: mean of triplicate light bottles); filled symbols represent the mean value for that station. The mean value for all samples is 0.81.

shown in Fig. 2. Uptake values ranged between  $0.001$  and  $0.1 \mu\text{mol Si L}^{-1} \text{ h}^{-1}$ , although most were  $0.005$  to  $0.05 \mu\text{mol Si L}^{-1} \text{ h}^{-1}$ . This is consistent with previous observations in coastal Northeast Atlantic studies (Paasche and Ostergren 1980; Kristiansen et al. 2000) and in spring bloom studies in other mesotrophic regions (e.g., Treguer et al. 1991; Brzezinski et al. 2001; Leynaert et al. 2001). In contrast to primary production, <sup>32</sup>Si uptake did not decrease to zero at the base of the photic zone. The high subsurface uptake rates frequently corresponded with increased nutrient concentrations at the thermocline, and at some stations (14000, 14005, 14060) increased particulate concentrations were also observed in this region of the water column (Table 2). The mean ratio of silica uptake between the dark and light paired samples was 0.8, indicating that silica uptake is at best loosely coupled to light availability, at least over a 6-h timescale (Fig. 3). Silica uptake in light-shielded samples has been observed previously, with dark:light uptake ratios from 0.4 to  $>1$  (Azam and Chisholm 1976; Nelson and Brzezinski 1997). No relationship was observed between the dark:light uptake ratio and either depth or ambient silica concentration in our samples.

Daily silica uptake rates were calculated by summing

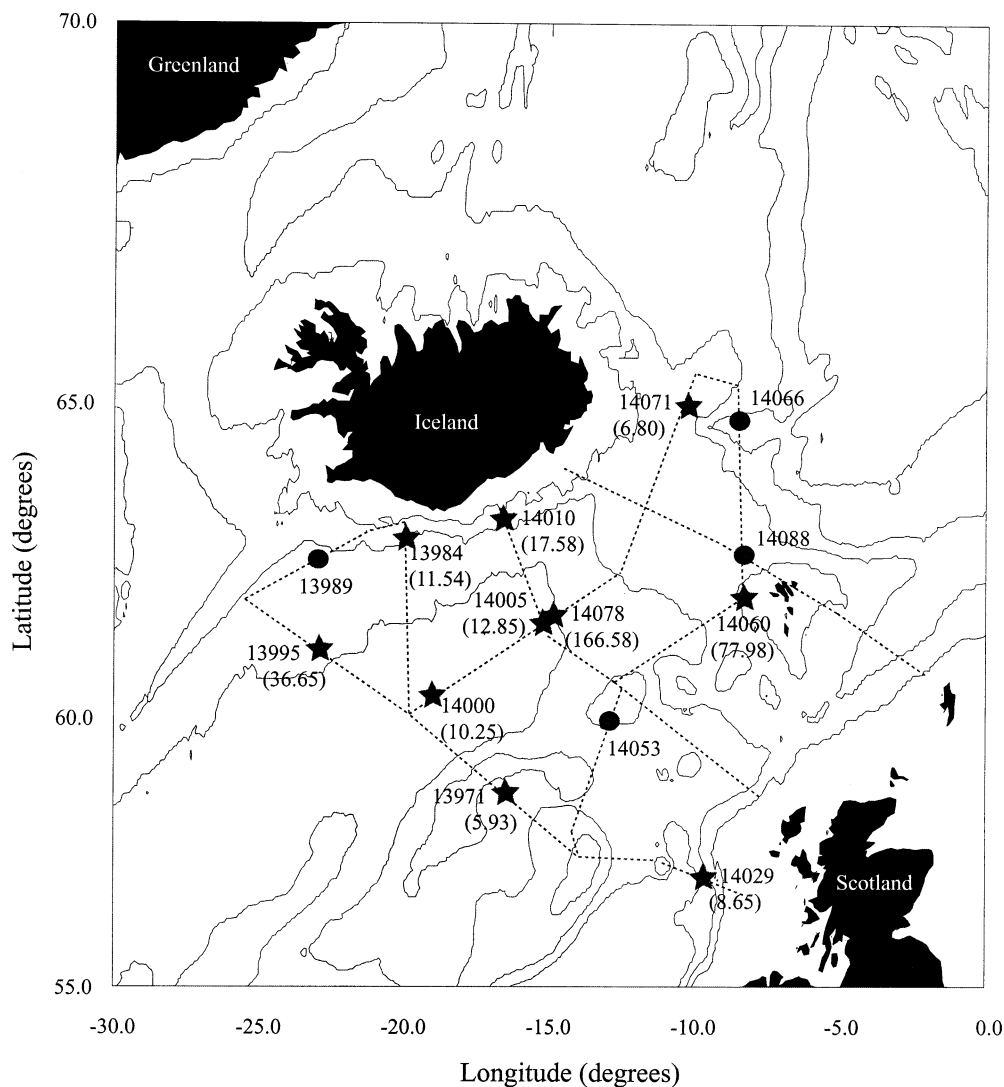


Fig. 4. Location of sampling stations for  $^{32}\text{Si}$  uptake studies (stars), showing the distribution of silica uptake rates in  $\text{mmol Si m}^{-2} \text{d}^{-1}$  integrated to the depth of 0.1% surface light intensity (in brackets). The daily rates were calculated incorporating both daylight and dark rates, as described in the text. Stations at which uptake kinetics experiments were carried out are also highlighted (circles), and the overall cruise track is marked as a dashed line.

twice the uptake of both the light and dark samples to give a value for the 12-h day–night cycle. Daily depth-integrated silica uptake rates at seven of the stations were between 5 and 20  $\text{mmol Si m}^{-2} \text{d}^{-1}$  (Fig. 4), similar to previous values reported for nonbloom uptake in HNLC regions (Brzezinski et al. 2001; Gall et al. 2001). At two stations, 14060 and 14078, silica uptake rates were 78  $\text{mmol Si m}^{-2} \text{d}^{-1}$  and 167  $\text{mmol Si m}^{-2} \text{d}^{-1}$ , respectively, nearly an order of magnitude greater than the other stations. Primary production at these stations was also among the highest observed on the cruise.

*Silica uptake dynamics during the progress of the spring bloom*—The integrated silica uptake rates did not vary in a consistent manner with either the date or location of sampling, and regression analysis of daily silica uptake rates with the same parameters as for primary production and with

primary productivity itself did not reveal any statistically significant relationships. It appears, therefore, that interpretation of the results with respect to the changing patterns of silica uptake as the spring bloom develops is hindered by the temporal, spatial, and hydrographic diversity of the stations. In order to fully understand the sequential changes in silica uptake dynamics in the Northeast Atlantic, it is necessary to establish an appropriate time series through which the development of the diatom spring bloom can be traced.

Following the observation of Kristiansen et al. (2000) that diatom growth rates declined as silica concentration decreased in a coastal North Atlantic spring diatom bloom, we synthesized a quasi-time series by ordering the results by mean photic zone silica concentration (a mean value being used in order to eliminate effects caused by variable photic depths). It has been observed previously, in both laboratory

(Claquin et al. 2002) and field (Brzezinski and Kosman 1996; Nelson and Brzezinski 1997; Brzezinski et al. 1998) studies, that the factors controlling primary production do not necessarily correspond with those that control silica uptake. Thus, while interaction between light regime, mixing depth, and nutrient concentrations may govern the initiation and species composition of the phytoplankton bloom, we believe that the degree of silica depletion is likely to be the simplest reliable indicator of the progression of the diatom phase of the spring bloom. This approach is subject to the following assumptions:

1. All water types covered by the FISHERS cruise had similar prebloom silica concentrations. Winter mixing to 600–800-m depth of silica-depleted surface water with deeper, more nutrient-rich water is primarily responsible for determining the prebloom silica concentration (Koeve 2001). Therefore, examination of the silica concentration at 400-m depth (or the bottom sampling depth if the station is shallower than 400 m) should give an indication of the prebloom silica concentration of the surface water. Silica concentrations at these depths were 6–7  $\mu\text{mol L}^{-1}$  for all stations, except 13971 (8.46  $\mu\text{mol L}^{-1}$ ), 14071 (9.87  $\mu\text{mol L}^{-1}$ ), and the Scottish shelf Sta. 14029 (4.47  $\mu\text{mol L}^{-1}$ ), suggesting this is a reasonable assumption for most sites.

2. The concentration of dissolved silica at all sites was not significantly affected by storm activity, mixing across the thermocline, or dissolution of diatom frustules in the surface layer during the period of the cruise.

We believe this approach is more useful than ordering the stations by alternative tracers of bloom progression, e.g., POC, BSi, Chl *a*, and fucoxanthin concentrations, or primary production rates. These latter parameters are state variables, which rise and fall as the bloom progresses and in some cases are also influenced by other phytoplankton production (POC, Chl *a*, primary production). In contrast, if the above assumptions are correct, silica concentration would be expected to decline throughout the entire period of the diatom bloom and, in addition, is related directly only to use by diatoms.

Figure 5a shows changes in average photic zone absolute silica uptake and specific uptake rates for the 10 silica uptake stations, ordered by decreasing depth-averaged photic zone silica concentrations. With the exception of Sta. 13995, it is apparent that peak rates of absolute uptake (Stas. 14060, 14078) occur only at silica concentrations greater than about 1–2  $\mu\text{mol L}^{-1}$ . Below this value, it appears that diatom growth is limited by substrate concentration, with mean integrated absolute uptake rates below 1  $\text{mmol m}^{-3} \text{d}^{-1}$  for stations where silica is below 2  $\mu\text{mol L}^{-1}$ .

Figure 5b shows depth-averaged photic zone primary production and depth-averaged chlorophyll plotted on the same basis as the silica parameters in Fig. 5a. No significant relationship existed between either parameter and silica concentration. In particular, peaks in both primary productivity and chlorophyll are observed at Stas. 14010 and 14029, where the depth-integrated silica concentration is low. No clear pattern emerges from ordering the biogenic particulate carbon or silica concentrations by depth-averaged photic zone silica concentrations (Fig. 5c) other than a general peak in both parameters at intermediate silica concentrations.

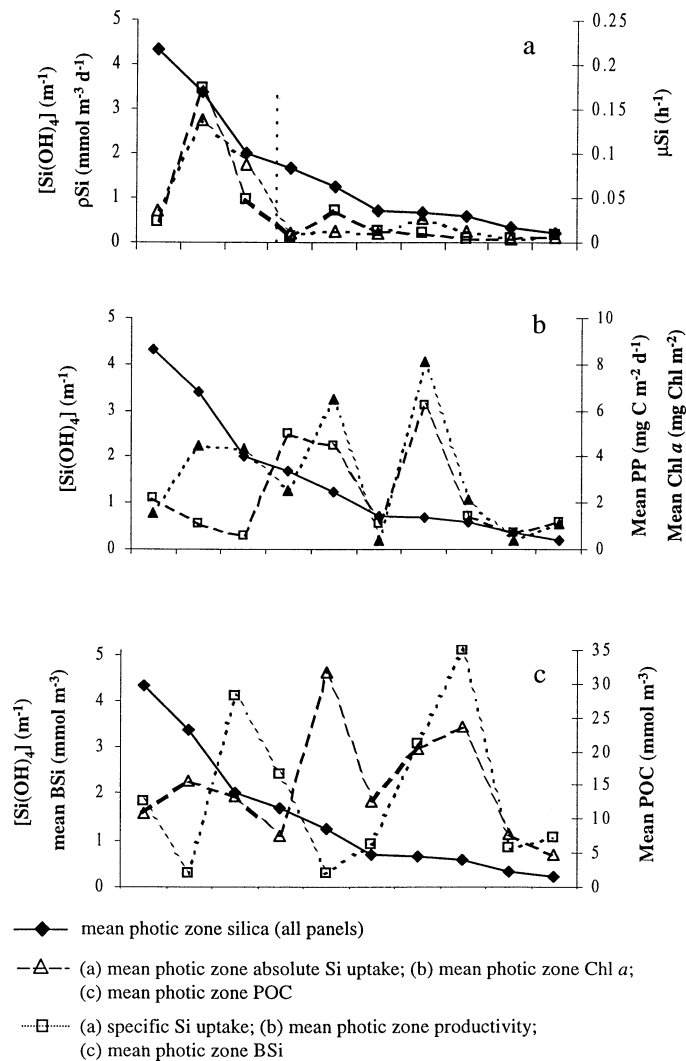


Fig. 5. The following data are presented here in order of mean photic zone silica concentration: (a) specific and depth-normalized absolute silica uptake; (b) depth-normalized absolute primary productivity and depth-normalized Chl *a*; (c) particulate organic carbon and biogenic silica concentrations.

**<sup>32</sup>Si uptake kinetics studies**—In all four silica uptake kinetics experiments, an approximately linear response of specific uptake to increased substrate concentration was observed (Fig. 6), with the  $r^2$  value for the best-fit line to the data being  $>0.9$  in all cases. The gradient of the slopes was variable: 0.001, 0.042, 0.0093, and 0.0037  $\text{h}^{-1} \mu\text{mol L}^{-1}$  for Stas. 13989 to 14088, respectively. Data regression was carried out to obtain both linear and hyperbolic fits to the data, and the goodness of fit and kinetic rate parameters thus obtained are shown in Table 3.

## Discussion

**Silica uptake dynamics during the progress of the spring bloom**—Ordering the silica uptake data by mean photic zone silica concentration appears to work well as a model for diatom bloom progression. Figure 5a demonstrates that peak

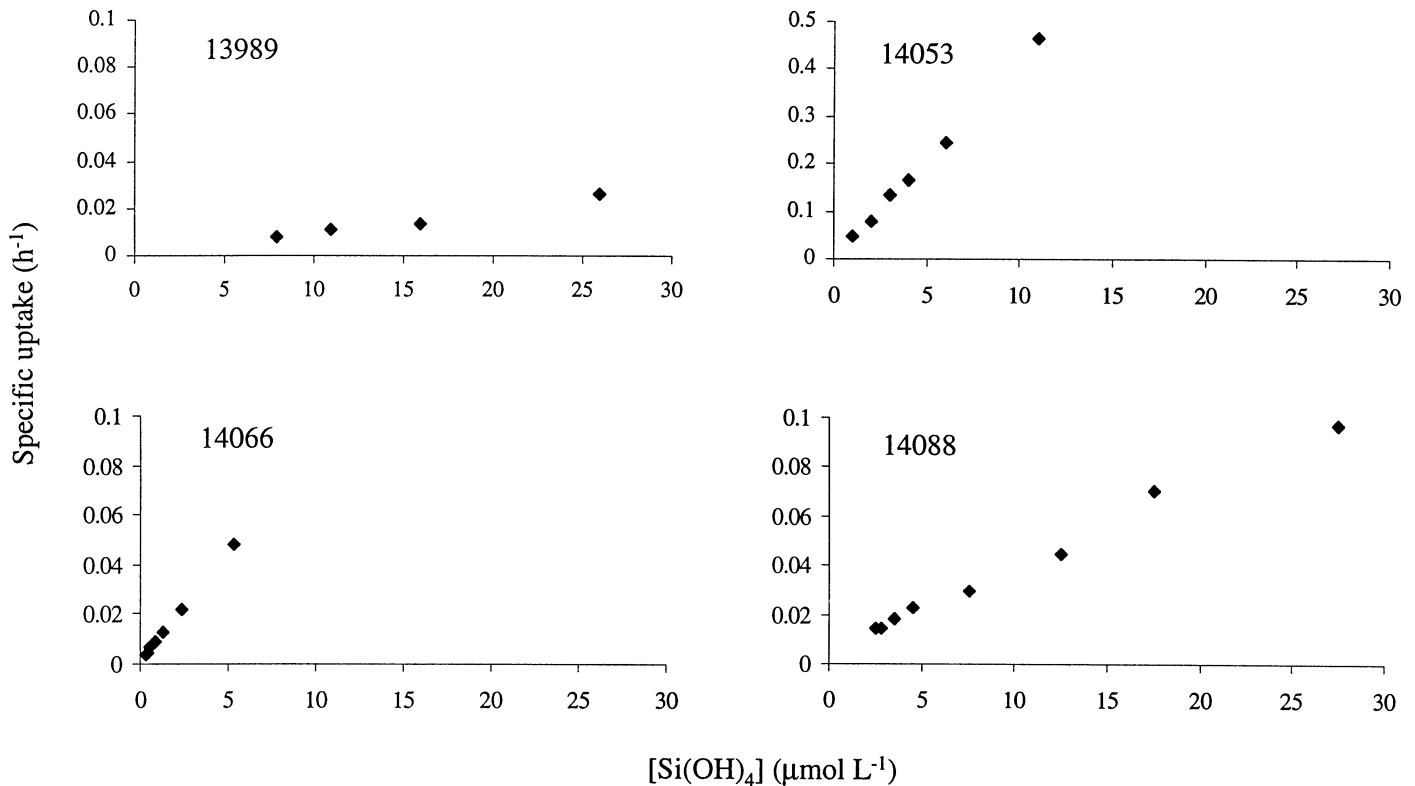


Fig. 6. Specific silicate uptake versus silicate concentration for uptake kinetics experiments; (a) 12 May, Sta. 13989, ambient surface silicate  $5.9 \mu\text{mol L}^{-1}$ ; (b) 23 May, Sta. 14053, ambient surface silicate  $1.0 \mu\text{mol L}^{-1}$ ; (c) 25 May, Sta. 14066, ambient surface silicate  $0.3 \mu\text{mol L}^{-1}$ ; (d) 29 May, Sta. 14088, ambient surface silicate  $2.5 \mu\text{mol L}^{-1}$ .

rates of absolute silica uptake (Stas. 14060, 14078) occur only where silica concentrations are greater than about  $1\text{--}2 \mu\text{mol L}^{-1}$ ; below this value, it appears that diatom growth is limited by substrate concentration. This observation agrees well with mesocosm experiments (Egge and Asknes 1992), which demonstrate that diatom dominance of a phytoplankton population decreased rapidly as concentrations fell below  $2 \mu\text{mol L}^{-1}$  Si. We therefore suggest that at those stations where depth-averaged photic zone silica is less than  $2 \mu\text{mol L}^{-1}$  Si, the spring diatom bloom had peaked and possibly begun to decline. At Sta. 13995, where the depth-averaged photic zone silica concentration was highest ( $4.3 \mu\text{mol L}^{-1}$ ), both primary production and biogenic silica concentrations were low; however, some depletion of surface silica relative

to deep waters was evident, indicating some diatom activity has occurred. This suggests conditions at Sta. 13995 represent a phase early in the diatom bloom and in the spring bloom in general.

When attempting to establish the temporal development of the phytoplankton bloom, it is clearly essential to consider concurrent changes in parameters other than silica concentration and uptake. Peaks in both primary productivity and chlorophyll are observed at Stas. 14010 and 14029 (Fig. 5b), where the mean photic zone silica concentration and uptake rates were low. The phytoplankton pigment data (Fig. 1) at these stations are dominated by chlorophyte and prymnesiophyte marker pigments, rather than those associated with diatoms. The low silica concentration at 14010 demonstrates

Table 3. Silica kinetic uptake parameters determined for NE Atlantic diatoms on FISHES cruise D258. Max  $[\text{Si}(\text{OH})_4]$  is the final concentration, in  $\mu\text{mol L}^{-1}$ , of silica in the most enriched bottle;  $V_{\text{max}}$  is the maximum specific uptake rate of silica of the diatom population;  $K_m$  is the concentration of silica at which  $V = 0.5V_{\text{max}}$ ;  $r^2$  is the least squares correlation coefficient of the hyperbolic fit (column 6) or linear fit (column 9) to the data;  $V_{\text{initial}}/V_{\text{max}}$  is the fraction of maximum recorded uptake occurring at ambient silica concentration; and slope is the gradient of the best fit straight line through the plot of  $V$  against  $[\text{Si}(\text{OH})_4]$ .

Station	Ambient $[\text{Si}(\text{OH})_4]$	Max $[\text{Si}(\text{OH})_4]$	Hyperbolic fit			Linear fit			
			$V_{\text{max}}$ ( $\text{h}^{-1}$ )	$K_m$ ( $\mu\text{mol L}^{-1}$ )	$r^2$	$V_{\text{initial}}/$ $V_{\text{max}}$	Slope ( $\text{h}^{-1} \mu\text{mol L}^{-1}$ )	$r^2$	$V_{\text{initial}}/$ $V_{\text{max}}$
13995	5.9	25	0.017	4.6	0.38	0.470	0.001	0.69	31.6
14053	1.0	6	11.2	261	0.03	0.004	0.042	0.99	10.4
14066	0.3	12	0.218	19.3	0.79	0.016	0.009	0.99	7.2
14088	2.5	27	0.246	46.2	0.71	0.057	0.004	0.97	14.8

that the diatom-dominated phase of the bloom had passed, although the phytoplankton still maintained a high level of productivity. In contrast, the concentration of silica at Sta. 14029 is high relative to nitrate and phosphate concentrations. It may be significant that this station, located on the Scottish Shelf, had a deep-water silica concentration well below that of the other stations ( $4.5 \mu\text{mol}$ , compared to about  $7 \mu\text{mol}$ ). It therefore follows that while photic zone silica concentrations appear to be a fairly reliable indicator of diatom bloom progress, the same does not hold for the development of the spring bloom as a whole.

Mean photic zone POC and BSi concentrations are generally highest in the middle of the series (Fig. 5c). This may lend further weight to our hypothesis that ordering the data by mean photic zone silica concentration is an effective means of representing the diatom bloom progression. We suggest the high midseries values correspond to postbloom biomass present in the surface layer of the ocean. Low BSi and POC concentrations at the start and end of the time series are assumed therefore to represent low prebloom biomass and subduction of biogenic material into deeper waters at the end of the bloom, respectively. The decrease in POC concentration at Sta. 14005 can be explained by the presence of an extremely shallow (10 m) surface mixed layer, suggesting that accumulated particulate material has already been subducted.

In summary, the general concurrence of high ( $>2 \mu\text{mol L}^{-1}$ ) surface silica availability and high absolute and specific silica uptake rates suggests that availability of dissolved silica is the primary control on diatom bloom evolution. However, the absence of a similar correlation between silica concentration and primary productivity clearly indicates that ambient silica concentration alone cannot be used as a monitor of the overall spring bloom. Specifically, low silica uptake may be observed under conditions of relatively high silica concentration if the light and hydrographic conditions are insufficient to initiate the bloom. Similarly, high primary productivity may be maintained under silica-depleted conditions by late bloom phase mixed or nondiatomaceous communities.

*Changes in Si uptake profiles throughout the diatom bloom*—Synthesis of the data into a quasi-time series on the basis of photic zone silica concentration appears to provide a reasonable basis for interpreting silica uptake rates determined during the survey. With this approach, the shapes of the silica uptake profiles at different stages of the time series (Fig. 2) and comparison with primary production profiles (Fig. 7) are here examined in order to address the second of our hypotheses on diatom bloom progression.

Initial consideration of the data indicated a lack of differentiation in profile shape at the different bloom stages. However, by superposing the depth of the surface mixed layer and the dissolved silica profile on to the data, it was apparent that where the euphotic depth exceeded the mixed layer depth, silica uptake increased in the nutrient-rich deeper waters. This trend was apparent at all stations except 13995, which, as outlined above, exhibited low primary productivity and high nutrient concentrations and was identified as being in the initial stages of the bloom. During this early bloom

stage, silica uptake was highest in the surface mixed layer and decreased to lower levels at depth. The dissolved silica concentration increases fairly rapidly, from about  $3 \mu\text{mol L}^{-1}$  Si at the surface to  $6 \mu\text{mol L}^{-1}$  Si at about 20 m, increasing more gradually thereafter across the thermocline. Primary productivity at this station demonstrated a classical light-limited profile. Under such conditions, diatom growth is likely to be fastest in the high irradiance surface waters, leading to the initial depletion of the surface silica reservoir. However, occurrence of peaks in both BSi concentration and the diatom marker pigment fucoxanthin within the photic zone but below the immediate surface indicate there is some decoupling of the silica and carbon uptake mechanisms, even at the early stage of the bloom.

Conditions at Stas. 14060 and 14078, which have high rates of both primary productivity and silica uptake, are considered to be representative of the peak diatom bloom. As silica concentration in the surface water decreases toward 1– $2 \mu\text{mol L}^{-1}$ , silica uptake by diatoms at this depth may also be expected to decrease, and the highest silica uptake rates will occur adjacent to the thermocline, where dissolved silica concentrations are higher. At Sta. 14060, both silica and carbon uptake were highest below the surface. Pigment (Fig. 1) and biomass (Table 2) data for this station indicate a strongly diatom-dominated community located at depth, which may be expected to control overall production; that is, at this station Si and C uptake are approximately in balance. In contrast, at Sta. 14078, carbon uptake is high at the surface while the silica uptake peaks at depth. Pigment data indicate a mixed community at this station, so that overall production is probably influenced by a number of phytoplankton taxa, including diatoms. The decoupling of cellular silica and carbon cycles in diatoms (Claquin et al. 2002) means that diatoms in the silica-depleted upper region of the water column may continue to be productive in terms of carbon, if their silica requirement can be fulfilled by some combination of current uptake and earlier luxury uptake under higher silica conditions (Hildebrand 2002). Thus, we suggest that, at Sta. 14078, heavily silica-depleted diatoms have sunk to the base of the photic zone and used the deep silica pool that exists here, while productivity in the upper water column is maintained by a combination of other phytoplankton and diatoms using intracellular silica pools.

The remaining stations appear to have passed the peak of diatom bloom. Stations 13971, 14000, 14005, and 14071 have reached the end of the phytoplankton, as well as diatom bloom. All nutrient concentrations were low, and, overall production was low and constant throughout the photic zone. The silica concentration was below  $1 \mu\text{mol L}^{-1}$ , and depletion extended below the thermocline, suggesting diatoms had used this pool in addition to the silica trapped above the thermocline. At the two remaining stations, 14010 and 14029, primary production was supported by non-diatom-dominated communities (Fig. 1). The low silica concentration at 14010 implies the diatom bloom had already peaked here, but the comparatively high silica concentration at 14029 may suggest that diatom growth at this site was restricted.

In accordance with our second hypothesis, it appears that where silica uptake is substrate limited by low surface water

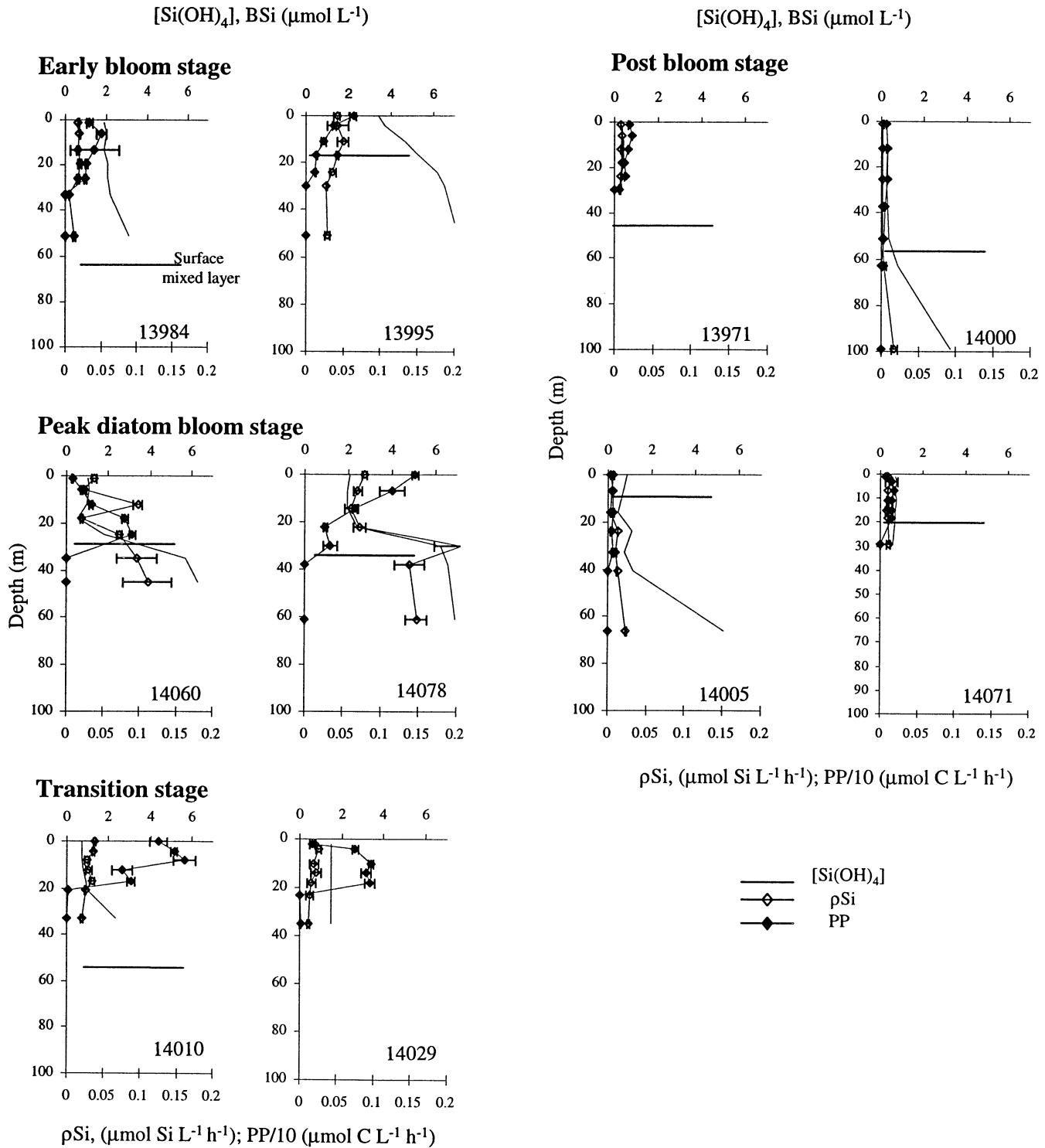


Fig. 7. Stations have been divided according to the phase of the spring bloom they appear to represent, based on the available uptake, nutrient, pigment, and biomass data. Early diatom bloom phase stage: reasonably high surface silica, low to moderate rates of production and silica uptake, silica uptake homogeneous throughout photic zone. Peak diatom bloom stage: high rates of silica uptake and primary productivity, surface silica depleted to 1–2  $\mu\text{mol L}^{-1}$ , intense silica uptake at thermocline boundary. Transition stage: silica uptake rates low, primary production high but driven by nondiatom community. Silica concentration variable depending on intensity of preceding bloom. Postbloom stage: low primary productivity and silica uptake rates, surface layer silica fully exhausted, POC and BSi concentrations typically highest below thermocline.

silica concentration, diatoms rapidly use the silica reservoir encountered at depth. The mechanism for silica uptake is generally considered to have both a low energy requirement and to be energized by respiration rather than photosynthesis (reviewed in Martin-Jezequel et al. 2000); therefore, in the short term at least, low irradiance is unlikely to hinder silica uptake. The faster sinking of nutrient-limited phytoplankton relative to their neutrally buoyant, nutrient-replete counterparts is also well documented (e.g., Bienfang et al. 1982; Brzezinski and Nelson 1988); thus, diatoms with the greatest silica requirement are transported to the area where the substrate is most available. This may account for the decoupling of the carbon and silica uptake profiles observed at many of the sites.

*Enrichment experiments*—Michaelis–Menten uptake kinetics predict a hyperbolic increase in biomass-specific uptake as substrate concentration increases. However, at all FISHERS stations at which uptake kinetics were derived, an approximately linear response of specific uptake rate to substrate concentration was observed (Fig. 6). Similar uptake kinetics have been obtained previously in tropical Atlantic oligotrophic waters (Brzezinski and Nelson 1996, silica additions up to  $6 \mu\text{mol L}^{-1}$ ) and the central North Pacific (Brzezinski et al. 1998, silica additions up to  $20 \mu\text{mol L}^{-1}$ ). However, in a Northeast Atlantic coastal study (Kristiansen et al. 2000), the diatom population exhibited Michaelis–Menten behavior. The uptake kinetics parameters derived by Kristiansen et al. (2000), under ambient silica concentrations of  $<0.1$  to  $6.3 \mu\text{mol L}^{-1}$ , gave values for the half-saturation constant,  $K_m$ , and the maximum rate of uptake,  $V_{\text{max}}$ , ranging from  $1.7$  to  $11.5 \mu\text{mol L}^{-1}$ , and  $6.9$  to  $26.7 \times 10^{-3} \text{ h}^{-1}$ , respectively. In general, the authors observed a positive correlation between both parameters and ambient silica concentration. The total silica added in the FISHERS experiments varied between  $6$  and  $27 \mu\text{mol L}^{-1}$ , depending on the ambient concentration, and, based on the study of Kristiansen et al. (2000), a Michaelis–Menten type response may have been expected.

Owing to the linear response of the FISHERS silica uptake kinetics, the data were interpreted following the approach of Brzezinski and Nelson (1996) for data from the Sargasso Sea. This is the only other study we are aware of that explicitly reports linear uptake kinetics. These authors used a linear regression to fit a straight line through zero to the data and compared the gradient of the slopes as an indicator of diatom response to substrate increase. The gradients obtained in the present study ranged from  $0.001$  to  $0.042 \text{ h}^{-1} \mu\text{mol L}^{-1}$  (Table 3), which compare favorably with the range of approximately  $0.001$ – $0.01 \text{ h}^{-1} \mu\text{mol L}^{-1}$  found in the Sargasso Sea (Brzezinski and Nelson 1996). No correlation between slope gradient and factors such as ambient silica concentration or primary productivity were observed in the FISHERS study. However, we observed that the lowest slope gradients corresponded to Stas. 13989 ( $0.001 \text{ h}^{-1}$ ) and 14088 ( $0.004 \text{ h}^{-1}$ ), where *Nitzschia delicatissima* composed over 90% of the total diatom assemblage. At Sta. 14066 (gradient  $0.01 \text{ h}^{-1}$ ), the species composition was approximately 50% each of *N. delicatissima* and *Chaetoceros decipiens*. The highest gradient at Sta. 14053 corresponded with a highly

diverse diatom assemblage. Some relationship between species composition and uptake kinetics may therefore be assumed.

An upper estimate of silica uptake efficiency was determined by using the silica uptake rate at the maximum addition of silica in the uptake experiments as a surrogate value for  $V_{\text{max}}$  (the maximum silica uptake rate observed by hyperbolic kinetics), here denoted by  $V_{\text{max}^*}$ . By taking the ratio of  $V_{\text{initial}}/V_{\text{max}^*}$ , where  $V_{\text{initial}}$  is the uptake rate at ambient silica concentrations, we can deduce that the uptake rate was less than 7%–15% of maximum possible rate for Stas. 14053, 14066, and 14088, and less than 32% for Sta. 13989. However, since no leveling off of the curves was observed, these figures must be taken as absolute maximum estimates of uptake efficiency.

It is necessary to consider the possibility that the linear data from the enrichment experiments represent the lower section of a hyperbolic curve and may be used to estimate the silica uptake kinetics parameters. A statistically significant hyperbolic fit to the data can only be obtained for Stas. 14066 and 14088 ( $r^2 > 0.7$ ); however, the level of significance is still less than that of the linear fit described above.  $V_{\text{max}}$  and  $K_m$ , the half-saturation constant, were calculated using a Woolf–Haines plot (Table 3). Both values were much greater than observed in the Oslofjord (Kristiansen et al. 2000), although comparably high values have been observed in the central North Pacific (Brzezinski et al. 1998). The  $V_{\text{initial}}/V_{\text{max}}$  ratio indicates that silica uptake at these two sites is limited to only 2% and 6% of the maximum observed rate, again comparable with values observed at some stations in the central North Pacific. However, the significantly better linear fit to the data demands that parameters determined from the forced hyperbolic fit be treated with caution.

Both the linear and hyperbolic approaches used in analysis of the kinetic uptake data indicate that the North Atlantic diatom populations appear to have low efficiency for silica uptake for typical values of surface silica concentration. As noted by Brzezinski and Nelson (1996), such severe silica limitation may be adaptive rather than detrimental, since silica limitation of growth is less damaging to the cell in the long term compared to limitation by other nutrients. While such reasoning may also account for the low silica uptake efficiencies at the ambient silica concentrations at the FISHERS stations, it does not explain why silica uptake can increase proportionally to substrate concentration over such a wide concentration range or why the theoretical  $V_{\text{max}}$  values observed at the FISHERS stations are so high. The observation of subsurface silica uptake maxima or significant uptake at depth at the FISHERS stations and in other oligotrophic and mesotrophic areas (Brzezinski and Kosman 1996; Brzezinski et al. 1998) may help explain this anomaly.

Diatom populations can maintain their growth rates under silica-limited conditions by thinning their frustules so that cellular C:Si and N:Si ratios may be three or four times their optimal value (e.g., Brzezinski et al. 1990); however, at some point the diatom will need to replenish its cellular Si content to maintain growth. The preferential sinking of nutrient-stressed diatoms has already been noted (Bienfang et al. 1982; Brzezinski and Nelson 1988), and for most open ocean diatoms, this would result in transport to deeper water

with higher nutrient concentrations—maximum deep-water silica concentrations in the Northeast Atlantic are 15–20  $\mu\text{mol L}^{-1}$ . A high  $V_{\text{max}}$ , well above the concentrations expected in surface waters, would enable diatoms to rapidly take up any silica encountered at depth or introduced by episodic mixing. This in turn would enable them to regulate their buoyancy quickly, thus limiting the likelihood of the cells being transported permanently out of the surface mixed layer of the ocean. As silica uptake has a relatively small energy requirement, maintaining the ability to take up silica rapidly costs the cell very little but has high potential benefit.

This study presents the first measurements of  $^{32}\text{Si}$  assimilation in the open Northeast Atlantic Ocean. Individual uptake rate measurements were generally of the same order of magnitude as previous studies in environments, such as the coastal Northeast Atlantic and the Southern Ocean. Some Northeast Atlantic silica uptake profiles exhibited subsurface maxima, as has also been observed in other mesotrophic and oligotrophic regions (Brzezinski and Kosman 1996; Nelson and Brzezinski 1997; Brzezinski et al. 1998). Frequently, the increased uptake corresponded with increased nutrient concentrations at the base of the surface mixed layer. This rapid uptake at increased nutrient concentrations was considered to be a response by diatoms to near exhaustion of the surface silica pool, which had become silica depleted due to rapid cell division. In most profiles, uptake was still observed at light levels of 0.1% surface PAR, and silica uptake was also noted in dark samples at rates of 40% to >100% of the comparable light uptake rate. This implies a low energy dependence of silica uptake and a decoupling of silica and carbon uptake rates by diatoms.

A dark uptake component was included in the final calculation of depth-integrated daily silica uptake rates. Seven out of the ten stations sampled had daily silica uptake rates in the range previously observed for Southern Ocean non-bloom production, but rates at two stations were higher than any previously reported values, at 78 and 166  $\text{mmol Si m}^{-2} \text{d}^{-1}$ . These stations were also sites of high primary productivity. Silica uptake rates were highly variable over space and time, and thus the data were considered on a quasi-time-series basis, using the mean photic zone silica concentration as a controlling parameter. This model appeared to successfully rationalize the data in terms of the progression of the diatom bloom, despite the wide range of hydrographic, biological, and biogeochemical conditions sampled. Overall, low absolute and specific silica uptake rates were observed at the beginning and end of the bloom, with high values at the bloom peak. Of particular note is that the data suggest Northeast Atlantic diatom silica uptake rates are low at silica concentrations below 2  $\mu\text{mol L}^{-1}$ , in accordance with the observation of Egge and Aksnes (1992) that diatoms dominate phytoplankton populations at concentrations above this limit. The model did not, however, trace the pattern of primary productivity distribution, underlining that the silica concentration model is applicable to the diatom-controlled phase of the bloom only.

Uptake kinetics studies demonstrated a linear relationship of silica uptake with substrate concentration at silica concentrations of up to 27  $\mu\text{mol L}^{-1}$ . A statistically significant Michaelis–Menten curve was fitted to data from two of the

stations, and  $V_{\text{max}}$  values on the order of 0.2  $\text{h}^{-1}$  and  $K_m$  of 19.1 and 46.2  $\mu\text{mol L}^{-1}$  were obtained. Regardless of whether this approach is used or a best-fit straight line is applied to the data, the uptake kinetics are inefficient compared to their potential maximum values. While this is surprising in an environment where ambient silica may be limiting to growth, there are possible benefits of silica limitation in terms of cell survival under nutrient-depleted conditions. Further, the high  $V_{\text{max}}$  value obtained indicates that Northeast Atlantic diatoms are capable of responding to pulsed inputs of nutrients and/or transport to zones of higher nutrient concentrations at the depth of the thermocline.

## References

- AZAM, F., AND S. W. CHISHOLM. 1976. Silicic acid uptake and incorporation by natural marine phytoplankton populations. *Limnol. Oceanogr.* **21**: 427–435.
- BARLOW, R. G., M. A. GOUGH, R. F. C. MANTOURA, AND T. W. FILEMAN. 1993. Pigment signatures of the phytoplankton composition in the northeastern Atlantic during the 1990 spring bloom. *Deep-Sea Res.* **40**: 459–477.
- BIENFANG, P. K., P. J. HARRISON, AND L. M. QUARMBY. 1982. Sinking rate response to depletion of nitrate, phosphate and silica in four marine diatoms. *Mar. Biol.* **67**: 295–302.
- BOYD, P., J. LAROCHE, M. GALL, R. FREW, AND M. L. MCKAY. 1999. Role of iron, light and silicate in controlling algal biomass in subantarctic waters SE of New Zealand. *J. Geophys. Res.* **104**: 13395–13408.
- BRZEZINSKI, M. A. 1985. The Si:C:N ratio of marine diatoms: Interspecific variability and the effect of some environmental variables. *J. Phycol.* **21**: 347–357.
- , AND C. A. KOSMAN. 1996. Silica production in the Sargasso Sea during spring 1989. *Mar. Ecol. Prog. Ser.* **142**: 39–45.
- , AND D. M. NELSON. 1988. Differential cell sinking as a factor influencing diatom species competition for limiting nutrients. *J. Exp. Mar. Biol. Ecol.* **119**: 179–200.
- , AND ———. 1996. Chronic substrate limitation of silicic acid uptake rates in the western Sargasso Sea. *Deep-Sea Res.* **43**: 437–453.
- , ———, V. M. FRANCK, AND D. E. SIGMON. 2001. Silicon dynamics within an intense open-ocean diatom bloom in the Pacific sector of the Southern Ocean. *Deep-Sea Res. II* **48**: 3997–4018.
- , R. J. OLSON, AND S. W. CHISHOLM. 1990. Silicon availability and cell-cycle progression in marine diatoms. *Mar. Ecol. Prog. Ser.* **67**: 83–96.
- , AND D. R. PHILLIPS. 1997. Evaluation of Si-32 as a tracer for measuring silica production rates in marine waters. *Limnol. Oceanogr.* **42**: 856–865.
- , ———, F. P. CHAVEZ, G. E. FRIEDERICH, AND R. C. DUGDALE. 1997. Silica production in the Monterey, California, upwelling system. *Limnol. Oceanogr.* **42**: 1694–1705.
- , T. A. VILLAREAL, AND F. LIPSCHULTZ. 1998. Silica production and the contribution of diatoms to new and primary production in the central North Pacific. *Mar. Ecol. Prog. Ser.* **167**: 89–104.
- CLAQUIN, P., V. MARTIN-JEZEQUEL, J. C. KROMKAMP, M. J. W. VELDHUIS, AND G. W. KRAAY. 2002. Uncoupling of silicon compared with carbon and nitrogen metabolisms and the role of the cell cycle in continuous cultures of *Thalassiosira pseudonana* (bacillariophyceae) under light, nitrogen and phosphorus control. *J. Phycol.* **38**: 922–930.

- DUCKLOW, H. W., AND R. P. HARRIS. 1993. Introduction to the JGOFS North-Atlantic bloom experiment. *Deep-Sea Res. II* **40**: 1–8.
- EGGE, J. K., AND D. L. AKSNES. 1992. Silicate as regulating nutrient in phytoplankton competition. *Mar. Ecol. Prog. Ser.* **83**: 281–289.
- FRANCK, V. M., M. A. BRZEZINSKI, K. H. COALE, AND D. M. NELSON. 2000. Iron and silicic acid concentrations regulate Si uptake north and south of the Polar Frontal Zone in the Pacific Sector of the Southern Ocean. *Deep-Sea Res. II* **47**: 3315–3338.
- GALL, M. P., R. STRZEPEK, M. MALDONADO, AND P. W. BOYD. 2001. Phytoplankton processes. Part 2. Rates of primary production and factors controlling algal growth during the Southern Ocean Iron Release Experiment (SOIREE) *Deep-Sea Res. II* **48**: 2571–2590.
- HILDEBRAND, M. 2002. Lack of coupling between silicon and other elemental metabolisms in diatoms. *J. Phycol.* **38**: 841–843.
- HONJO, S., AND S. J. MANGANINI. 1993. Annual biogenic particle fluxes to the interior of the North Atlantic Ocean studied at 34-degrees N 21-degrees W and 48 degrees N 21 degrees W. *Deep-Sea Res. II* **40**: 587–607.
- JEFFREY, S. W., AND M. VESK. 1997. Introduction to marine phytoplankton and their pigment signatures. In S. W. Jeffrey, R. F. C. Mantoura, and S. W. Wright [eds.], *Phytoplankton pigments in oceanography*. Unesco Publishing.
- KIRKWOOD, D. S. 1995. The SanPlus segmented flow autoanalyser and its applications. Skalar Analytical BV publication.
- KOEVE, W. 2001. Wintertime nutrients in the North Atlantic—new approaches and implications for new production estimates. *Mar. Chem.* **74**: 245–260.
- KRISTIANSEN, S., T. FARROT, AND L.-J. NAUSTVOLL. 2000. Production of biogenic silica by spring diatoms. *Limnol. Oceanogr.* **45**: 472–478.
- LEYNAERT, A., P. TREGUER, C. LANCELOT, AND M. RODIER. 2001. Silicon limitation of biogenic silica production in the Equatorial Pacific. *Deep-Sea Res. I* **48**: 639–660.
- LOUANCHI, F., AND R. G. NAJJAR. 2001. Annual cycles of nutrients and oxygen in the upper layers of the North Atlantic Ocean. *Deep-Sea Res. II* **48**: 2155–2171.
- MARTIN-JEZEQUEL, V., M. HILDEBRAND, AND M. A. BRZEZINSKI. 2000. Silicon metabolism in diatoms: Implications for growth. *J. Phycol.* **36**: 821–840.
- NELSON, D. M., AND M. A. BRZEZINSKI. 1990. Kinetics of silicic acid uptake by natural diatom assemblages in 2 Gulf Stream warm core rings. *Mar. Ecol. Prog. Ser.* **62**: 283–292.
- , AND ———. 1997. Diatom growth and productivity in an oligotrophic midocean gyre: A 3-yr record from the Sargasso Sea near Bermuda. *Limnol. Oceanogr.* **42**: 473–486.
- , ———, D. E. SIGMON, AND V. M. FRANCK. 2001. A seasonal progression of Si limitation in the Pacific sector of the Southern Ocean. *Deep-Sea Res. II* **48**: 3973–3995.
- , AND J. J. GOERING. 1977. A stable isotope tracer method to measure silicic acid uptake by marine phytoplankton. *Anal. Biochem.* **78**: 139–147.
- , AND ———. 1978. Assimilation of silicic acid by phytoplankton in the Baja California and Northwest Africa upwelling systems. *Limnol. Oceanogr.* **23**: 508–517.
- PAASCHE, E., AND I. OSTERGREN. 1980. The annual cycle of plankton diatom growth and silica production in the inner Oslofjord. *Limnol. Oceanogr.* **25**: 481–494.
- PARSONS, T. R., Y. MAITA, AND C. M. LALLI. 1984. A manual of chemical and biological methods for seawater analysis. Pergamon Press.
- PONDAVEN, P., D. RUIZ-PINO, J. N. DRUON, C. FRAVALO, AND P. TREGUER. 1999. Factors controlling silicon and nitrogen biogeochemical cycles in high nutrient low chlorophyll systems (the Southern Ocean and the North Pacific): Comparison with a mesotrophic system (the North Atlantic). *Deep-Sea Res. I* **46**: 1923–1968.
- QUEGUINER, B., AND M. A. BRZEZINSKI. 2002. Biogenic silica production rates and particulate organic matter distribution in the Atlantic sector of the Southern Ocean during austral spring 1992. *Deep-Sea Res. II* **49**: 1765–1786.
- RAGUENEAU, O., AND P. TREGUER. 1994. Determination of silica in coastal waters—applicability and limits of the alkaline digestion method. *Mar. Chem.* **45**: 43–51.
- SANDERS, R., AND T. JICKELS. 2000. Total organic nutrients in Drake Passage. *Deep-Sea Res. I* **47**: 997–1014.
- SAVIDGE, G., P. W. BOYD, A. J. POMROY, D. HARBOUR, AND I. JOINT. 1995. A study of the spring bloom in the N-E Atlantic Ocean in 1990. *Deep-Sea Res. I* **42**: 599–617.
- SMITH, W. O., D. M. NELSON, AND S. MATHOT. 1999. Phytoplankton growth rates in the Ross Sea, Antarctica, determined by independent methods: Temporal variations. *J. Plankton Res.* **21**: 1519–1536.
- TREGUER, P., L. LINDNER, A. J. VANBENNEKOM, A. LEYNAERY, M. PANOUSE, AND G. JAQUES. 1991. Production of biogenic silica in the Weddell-Scotia Seas measured with Si-32. *Limnol. Oceanogr.* **36**: 1217–1227.
- WELSCHMEYER, N. A. 1994. Fluorometric analysis of chlorophyll *a* in the presence of chlorophyll-*b* and phaeopigments. *Limnol. Oceanogr.* **39**: 1985–1992.

Received: 8 October 2002

Accepted: 26 February 2003

Amended: 18 March 2003